On analytical ballistic penetration fundamental model and design

JACOB NAGLER
NIRC,
Haifa, Givat Downes
ISRAEL

Abstract: - This paper presents a new fresh theoretical study of the ballistic penetration phenomena into hard materials due to low-energy bodies' motion. This model based on the energy balance between the kinetic energy of the piercing body and the protective body thermal energy. Following this equilibrium alongside the equation of the projectile motion, the resulting deceleration value is analytically calculated. Substituting the obtained deceleration value into the kinematic equilibrium results with the penetration thickness expression as well as the time of penetration inside the mono and multi layers materials (like, monolithic and composite materials). In addition, equivalently to the Johnson-Cook model, a proposed impact stress for penetrative and non-penetrative cases was developed. Additionally, a residual velocity expression alongside the evaluation of the total energy and deceleration parameters were also determined. Key parameters are the projectile effective length, which defines the projectile geometry alongside the material strength parameters (heat capacity, Yield, compressive and tensile strengths). Finally, good numerical agreement (order of magnitude and numerical values) has been found between various literature experimental tests and current analytic solution for the kinematic parameters.

Key-Words: Ballistic; penetration thickness; time of penetration; thermal energy; Deceleration; energy equilibrium; monolithic material; composite material; kinematic relations.

Received: March 20, 2021. Revised: September 25, 2021. Accepted: October 15, 2021. Published: October 20, 2021.

1 Introduction

The ballistic mechanisms of penetrating high-energy bodies (also known as projectile bodies) into another protective material body, have been studied widely by many researches [1-52]. Our discussion will be limited (experimental comparison) especially to hard armor materials with some touch to hyper elastic/soft materials while the projectile body is relatively small compared to the armor length (about at least 1/3 ratio). In addition, the projectile geometry shape will mainly be considered here as bullet conical body. Simple scheme for composite armor will be introduced continually, as well as for monolayer shield component. The analytic solution development based on stress-strain energetic terms together with kinematic relations.

Initially, to calculate the armor thickness, Dr. Louis Thompson from the U.S. Naval [1-2] has developed a formula (named after him: "Thompson – F formula") based on comparison between the projectile (also called 'bullet' in weapon terms) kinetic energy and the work done by the bullet. The formula is simply dependent on the projectile data: diameter, mass, velocity and dimensionless factor. Later on, new modulations of this formula have been proposed in the recent years by by Okun [3].

An effort to make more accurate formulations in order to evaluate the penetration thickness by making better understanding about the relation between the armor material science and the energy physics, has been performed later by Smith et al. [4, 5]. The latter studies have been concentrated on understanding the projectile impact effect on the armor textile yarns by evaluating critical velocities and wave propagation due to the impact effect using stress-strain analytic mechanical relationships. About one decade later, an alternative numerical model containing the impact deformation and time of penetration suggested by Wilkins [6]. One year later (1979), Kar [7] has found the penetration thickness formulation dependent on the projectile diameters alongside other penetration and shape factors (e.g., shield material ultimate static tensile strength and energy term). The last factors were relatively new in the field while have been found experimentally and by using the residual velocity theory. During a decade later, advanced experimental research on materials subjected to large strains combined with high temperatures exhibiting the basics of dynamics impact theory have been performed by Johnson [8] and Zukas [9], respectively.

In 1994, Stone [11] has proposed a new kinetic approach involved with semi-empirical relations based on the study of Allen et al. [10]. In this method [11] a general equation of the ballistic projectile motion was developed while dependent on the acting forces as function of the velocity (e.g. fluid dynamics drag, kinetic friction on the surface, deceleration coefficient due to the inherent structural properties) representing the developed deceleration. Using this method he distincted between hard and soft materials by assuming that in case of hard armor materials, the coefficient of the fluid drag and the kinetic friction become zero (in our model it will be equivalent to the friction energy and the drag energy terms). In addition, in case of viscous materials (like sand, gel, etc.) only the fluid drag might be neglected compared to inviscid materials (like armor with gas hollows), where only the friction coefficient should be neglected.

Another kind of materials are called soft materials (like liquids) in which the material friction is neglected (strain and stress friction effects). Yet, Stone [11] has also mentioned an integrated type model, known as controlled armor materials where all coefficients are participated (ballistic gelatin, supersaturated soils, etc.). The current essay presents an equivalent theoretical presentative model that expressed in energetic and kinetic terms for the process of projectile penetration into armor.

As mentioned in the previous paragraph, the armor hardness (or toughness) type definition to be 'hard' or 'soft' is determined by the stress-strain relations as well as other accompanied parameters (density, compressive strength and high elastic modulus, tensile strength that might be low for ceramics case) [10, 11]. To achieve the previous mentioned desired features, the armor should be produced from monolayers or being composed of several multi-layers [12 - 26].

Next generation of impact and penetration numerical modelling for all kind of materials were based on advanced detailed balanced scheme between the projectile kinetic energy, the absorbed work and the stress-strain energy mechanisms to evaluate the penetration thickness and the penetration time [12-26]. It is important to mention that the main mechanical effects that were examined in those studies [12-26] are as follows; the impact velocity and stress, while here alternative interpretation is modelled to asses some ballistic parameters, based on the extended energetic balance expression (e.g. thermal energy resistance) together with kinematic relations.

Following Stone studies, several analytic studies have proposed full model for the penetration formula based on the projectile kinematic equation of motion using stress-strain relations. The current brief would not be complete without mentioning the penetration formulas that have been developed by Yarin et al. [27], Ben-Dor et al. [28], Piekutowski et al. [29] Rosenberg & Dekel [30-32], Yossifon et al. [33], Børvik et al. [34-35] and Senthil et al. [36]. All mentioned equations are well summarized and compared in relative to experimental test by Stewart & Netherton [37]. Moreover, most formulations development have not considered the melting temperature in relative to the surrounding temperature, as introduced here, excluding the studies performed by [8, 22, 36, 38] that assuming the Johnson-Cook model [54-55]. In experimental sense, these study main results will be compared to some distinguished experiments (including finite element methods (FEM) simulations) [6, 19, 29, 33-36, 38-39, 41-42, 63].

The advantage of the following model is to have simple and completed analytic model proposes first ballistic approximate evaluations based on the traditional energetic balance involved with kinematic relations that easy to compare with experiments data by inserting several input parameters.

To sum it up, we will concentrate on simple analytic development that considers the thermal energy barrier that the projectile body should overcome in order to penetrate the protective body material (plugging mode) dependent mainly on the heat capacity, protective material density, the melting temperature and the protective material strength. As will be exhibited, the most dominant and crucial factor contribution to the deceleration of the projectile body is derived by the material heat loading followed by the material strength parameter. The current model will be developed for monolithic and composite materials. The main approximate formulations will be developed for penetration thickness, projectile deceleration, time of penetration, impact stress and the residual velocity compared to recent various experimental ballistic tests.

2 Problem Formulation

We consider here a conical projectile mass-body (with different geometry shape options) that moves vertically (neglecting the rotational velocity) towards an armor target through number of layers (composite or mono layer options) with appropriate entrance and exit velocities in each layer, while the *x-y* Cartesian axes origin are laid on the first layer as appear in Fig. 1. The projectile mass is considered

constant and the geometry diameter of the projectile body to armor ratio will be limited to the minimum ratio 1:3. The energy balance of the armor relative to the bullet motion (for convenience we will use the word 'bullet' to illustrate any penetrative body; for more shapes (appear in Fig. 1) – ogive, hemispherical, flat and conical, see Abtew *et al*. [24]) includes the bullet kinetic energy (E_k) as an input whereas the observed energy are the armor elastic strain energy ($E_{strain,A}$), compressive energy ($E_{compress,A}$), tensile plastic energy (using ultimate stress) ($E_{UTS,A}$), heat (Q_A) and friction surface work-energy (surface quality finish – roughness measurement) ($E_{friction}$) and drag work-energy (E_{Drag}), respectively. The energy balance, indeed, will model the impact, without using explicitly the ballistic equation of motion.

The representative energy balance in a general multi-stage formula is:

$$\Delta E^i = E_k^i - \left(\underbrace{Q^i + E_{strain,A}^i + E_{compress,A}^i + E_{UTS,A}^i + E_{friction}^i + E_{Drag}^i}_{E_{material\ energy-potential,A}^i} \right) = E_{k,p}^i = \frac{1}{2} m_b \left(v_p^i\right)^2, i = 1,2,..,N \quad (1)$$

whereas in the case of mono-layer $i = 1$. Remark that $E_{k,p}^i$ is the penetration kinetic energy in each time step (Δt), with the appropriate range of penetration velocities (v_p) ranging from v_{p0}^i representing the initial penetration velocity when the projectile cap (head characteristic length) enters the target *i*-layer until it arrives to the ending –*i* layer with the appropriate velocity v_{pf}^i, representing the emerging from the target *i*-layer, respectively. Here, for approximation purpose, we will concentrate on the initial penetration value (v_{p0}^i) to obtain finite and constant acceleration value at each layer. The projectile impact velocity (v_b^i) joins to the previous mentioned (each layer) penetration velocities (v_{p0}^i, v_{pf}^i) to complete the three main velocities that characterized the penetration process of each layer whereas the penetration time step difference of each layer will be noted by Δt^i. Accordingly, if the projectile stops its penetration motion in the *N* layer, then $v_{pf}^i = 0$, otherwise, if perforation occurs, the drag force only influences the projectile deceleration. One should notify that there are states in the multilayer armor when $v_b^{i=N} = v_{pf}^{i=N-1}$ (it also might be equal to zero). Usually, in the monolayer case, where $v_{p0}^i \neq 0$ the energy balance will enable an initial motion of projectile penetration. Of course, there are cases when $v_{p0}^i = v_{pf}^i = 0$ as the projectile stops at the beginning of its penetration into the *i*- layer.

As will be elaborated continually, in the current paper, we will assume that each layer has a single constant deceleration (a_i) value that corresponds to a single constant v_{p0}^i velocity value. The approximation assumes that the acceleration is constant until the projectile stops (or released) due to the armor material strength resistance such as the obtained approximated time steps will be shorter than the actual ones (experiments) but still in the same order, as will be discussed in Sec. 3).

Now, using Newton's second law, we know that the projectile work energy in each layer is equal to $W^i = m_b a^i P_d^i$ and therefore the total energy balance supplys:

$$W^i = m_b a^i P_d^i = \Delta E^i = E_k^i - (Q^i + E_{strain,A}^i + E_{compress,A}^i + E_{UTS,A}^i + E_{friction}^i + E_{Drag}^i) \quad (2)$$

2.1 *Monolithic Mono – layer penetration distance model*

The obtained generalized approximate expression that derived from Eq. (2) for the deceleration (a) of the projectile in the armor mono-layer will be:

$$a = \frac{\Delta E^{i=1}}{m_b \mathrm{P}_d} = \frac{\Delta E^{i=1}}{\rho_b \mathrm{V}_b \mathrm{P}_d} = \frac{\Delta E^{i=1}}{\rho_b \mathrm{S}_b L_b \mathrm{P_d}} = \frac{\frac{m_b v_b^2}{2} - \frac{E_A \varepsilon_A^2}{2} \mathrm{V}_A - m_A C_{P_A} \Delta T_A - \frac{1}{2}\sigma_{c_A} \varepsilon_{C,A}^2 \mathrm{V}_A - \frac{1}{2}\sigma_{UTS,A} \varepsilon_{plastic,A}^2 \mathrm{V}_A - 2\mu_k m_b g \mathrm{P}_d - \frac{1}{2} G_A \varepsilon_{shear,A}^2 \mathrm{V}_A - \frac{1}{2}\rho_b C_{D_b} S_b' v_b^2 \mathrm{P}_d}{\rho_b \mathrm{S}_b L_b \mathrm{P}_d} = \cdots$$

$$= \frac{v_b^2}{2P_d} - \frac{\rho_A C_{P_A} \Delta T_A + \frac{1}{2} E_A \varepsilon_A^2 + \frac{1}{2} \sigma_{c_A} \varepsilon_{C,A}^2 + \frac{1}{2} \sigma_{UTS,A} \varepsilon_{plastic,A}^2 + 2\mu_k \rho_b g L_b + \frac{1}{2} G_A \varepsilon_{shear,A}^2 + \frac{1 S_b'}{2 S_b} \rho_b C_{D_b} v_b^2}{\rho_b L_b} \quad (3)$$

Equation (3) was divided by the effective mass volumetric value (V_b) since the projectile mass fulfils $m_b = \rho_b V_b, V_b = S_b L_b, m_A = \rho_A V_A = \rho_A S_b P_d$ where $\rho_b, v_b, L_b, S_b, S_b', C_{D_b}$ are the density of the projectile head (lead cap, in case of particle – spherical radius), its velocity in the entrance of the armor, the bullet head (effective) characteristic length (based on the model produced by Yarin *et al*. [26] and Rosenberg & Dekel [30]), projectile base-diameter area, surface area and drag coefficient, respectively. The characteristic length is dependent on the projectile shape head (the head geometric obliquity) that is defined by (See Fig. 1):

$$L_b = L_0 + L(1-\varepsilon), \ \varepsilon = \frac{A_{front}}{A_{rear}};$$

Cylindrical flat ended cap (zero obliquity):

$\varepsilon = 1, \ L_b = L_0 = 2[mm]$

Cylindrical oblique ended cap:

$\varepsilon = \left(d_{front} / d_{rear}\right)^2, L_0 = 0[mm],$

$L_b = \left[1 - \left(d_{front} / d_{rear}\right)^2\right] L$

Cylindrical sharp cone:

$\varepsilon = 0, L_0 = 0[mm], L_b = L$

Spherical erosion particle:

$L = R, L_b = L/2$

(4)

Note that in the case of the cylindrical flat-ended cap (zero obliquity), the initial value of the projectile effective length is about 2 [mm] due to the participation of the geometrical edges during the impact process.

Also, $V_A, \rho_A, C_{P_A}, \Delta T_A = \left|T_{surr,b} - T_{meltingA}\right|, \sigma_{c_A}, \sigma_{UTS,A}, \varepsilon_{C,A}, G_A, \varepsilon_{shear,A}, \varepsilon_{plastic,A}$ represent the armor removal volume due to the projectile movement, mono layer density, heat capacity, the difference between the armor melting temperature and the surrounding temperature, armor compression limit stress, ultimate tensile strength, armor shear modulus and their appropriate compression including shear and plastic strains, respectively. The value for the surrounding temperature is dependent on the projectile temperature ($T_{surr,b}$) where $T_{surr,b} = T_0 + \frac{1}{2}\frac{v_b^2}{C_{P_b}}$ (obtained thanks to the kinetic balance $\frac{1}{2} m_b v_b^2$), here $T_0 = 293[K]$. Remark that in case of small particles (microns and below) we can use the temperature Boltzmann relation ($\frac{1}{2} m_b v_b^2 = \frac{3}{2} k_B T$) where the resulting temperature parameter can be expressed by $T = \frac{m_b v_b^2}{3 k_B}$. Note that g represents the gravity acceleration and μ_k is the armor surface finish kinetic friction coefficient (in the upper and lower projectile surfaces). Usually, the obtained values of the friction and drag work terms are lowerwith respect to the other energy terms values and therefore should be neglected.

The rationale behind the deceleration (3) formula is that it expresses the energy distribution over the effective bullet mass (m_b) multiplied by the penetration length (P_d) that responsible for the penetrative action against the armor material strength.

Accordingly, neglecting friction and drag force, resulting with deceleration expression due to energy balance that is assumed acting over the bullet course. Moreover, in case of brittle materials with low strain values, Eq. (3) turns to be $a = \frac{\Delta E^{i=1}}{m_b P_d} = \frac{v_b^2}{2P_d} - \frac{\rho_A C_{P_A} \Delta T_A + \frac{1}{2} \sigma_{c_A} \varepsilon_{C,A}^2 + 2\mu_k \rho_b g L_b + \frac{1 S_b'}{2 S_b} \rho_b C_{D_b} v_b^2}{\rho_b L_b}$. The thickness penetration value (P_d) for the monolayer is assumed to vary according the simple kinematic relation with inverse proportion to the bullet deceleration:

$$P_d = \left(v_b^2 - v_{pf}^2\right)/2a \quad (5)$$

Note that the v_p velocity expressions that could be considered as the residual velocity for any given armor plate thickness, are also evaluated

analytically as shown in Refs. [14, 51-52]. In the case of projectile full stop inside the armor, the penetrated velocity becomes zero ($v_{pf}=0$), to obtain:

$$\mathrm{P}_d = v_b^2/2a \tag{6}$$

Substituting relation (1) into Eq. (5) might lead the following expression representing the penetration distance (being dependent on the initial bullet initial velocity), in the form:

$$\mathrm{P}_d = \frac{2v_b^2\rho_b L_b}{\rho_A C_{P_A}\Delta T_A+\frac{1}{2}E_A\varepsilon_A^2+\frac{1}{2}\sigma_{c_A}\varepsilon_{C,A}^2+\frac{1}{2}\sigma_{UTS,A}\varepsilon_{plastic,A}^2+2\mu_k\rho_b g L_b +\frac{1}{2}G_A\varepsilon_{shear,A}^2+\frac{1S_b'}{2S_b}\rho_b C_{D_b}v_b^2} \tag{7}$$

Neglecting the air drag resistance, simply yielding:

$$\mathrm{P}_d = \frac{2v_b^2\rho_b L_b}{\rho_A C_{P_A}\Delta T_A+\frac{1}{2}E_A\varepsilon_A^2+\frac{1}{2}\sigma_{c_A}\varepsilon_{C,A}^2+\frac{1}{2}\sigma_{UTS,A}\varepsilon_{plastic,A}^2+2\mu_k\rho_b g L_b+\frac{1}{2}G_A\varepsilon_{shear,A}^2} \tag{8}$$

Also, the time of penetration ($\mathrm{t}_{penetration}$) for the mono-layer will be simply defined by the linear kinematic relation:

$$t_{penetration} = v_b\ /a \tag{9}$$

Remark that in case of projectile particles penetration model, the penetrative surface contact (average shape) area should be accounted simply with semi-circular geometry.

Reordering (5), lead to the residual velocity (v_{pf}) expression in the case of perforated armor test as:

$$v_{pf}^2 = v_b^2 - 2a\mathrm{P}_d = v_b^2 - 2\frac{\Delta E^{i=1}}{m_b} = \left(\frac{\rho_A C_{P_A}\Delta T_A+\frac{1}{2}E_A\varepsilon_A^2+\frac{1}{2}\sigma_{c_A}\varepsilon_{C,A}^2+\frac{1}{2}\sigma_{UTS,A}\varepsilon_{plastic,A}^2+2\mu_k\rho_b g L_b +\frac{1}{2}G_A\varepsilon_{shear,A}^2+\frac{1S_b'}{2S_b}\rho_b C_{D_b}v_b^2}{\rho_b L_b}\right)\mathrm{P}_d \tag{10}$$

whereas P_d and a parameters represent distance and deceleration, respectively, at the stage when the projectile emerges from the target first layer [53]. Note that by rearranging (9), the useful kinetic relation $\Delta E^{i=1} = m_b\left(\frac{v_b^2-v_p^2}{2}\right)$ is obtained.

Alternative time dependent residual velocity definition (useful for experiments [64]) might be calculated accordingly,

$$v_p = v_b - at = v_b - \frac{\Delta E^{i=1}}{m_b P_d}t = v_b - \frac{\Delta E^{i=1}}{m_b P_d}t = v_b - \left(\frac{\rho_A C_{P_A}\Delta T_A+\frac{1}{2}E_A\varepsilon_A^2+\frac{1}{2}\sigma_{c_A}\varepsilon_{C,A}^2+\frac{1}{2}\sigma_{UTS,A}\varepsilon_{plastic,A}^2+2\mu_k\rho_b g L_b +\frac{1}{2}G_A\varepsilon_{shear,A}^2+\frac{1S_b'}{2S_b}\rho_b C_{D_b}v_b^2}{\rho_b L_b}\right)t \tag{11}$$

In equivalent to Johnson-Cook model ([54] and its extension [55]), the equivalent stress will be:

$$\sigma_{Eq,NDM}^{i=1} = \frac{\Delta E^{i=1}}{S_b \mathrm{P}_d} \tag{12}$$

whereas in case of cylindrical projectile, the projectile surface area parameter is simply calculated by the well-known circle area formula $S_b = \frac{\pi d_{projectile}^2}{4}$. Substituting (1) into (12) leads to the following penetrative equivalent impact stress:

$$\sigma_{impact,NDM}^{i=1} = \frac{\frac{m_b v_b^2}{2} - \frac{E_A \varepsilon_A^2}{2} \mathrm{V}_A - m_A C_{P_A} \Delta T_A - \frac{1}{2}\sigma_{c_A}\varepsilon_{C,A}^2 \mathrm{V}_A - \frac{1}{2}\sigma_{UTS,A}\varepsilon_{plastic,A}^2 \mathrm{V}_A - 2\mu_k m_b g \mathrm{P}_d - \frac{1}{2} G_A \varepsilon_{shear,A}^2 \mathrm{V}_A - \frac{1}{2}\rho_b C_{D_b} S_b' v_b^2 P_d}{P_d S_b}$$
$$= \frac{\rho_b v_b^2}{2} - \rho_A C_{P_A} \Delta T_A - \frac{2\mu_k m_b g}{S_b} - \frac{1}{2} G_A \varepsilon_{shear,A}^2 - \frac{1}{2}\sigma_{UTS,A}\varepsilon_{plastic,A}^2 - \frac{1}{2}\sigma_{c_A}\varepsilon_{C,A}^2 - \frac{E_A \varepsilon_A^2}{2} - \frac{1}{2}\rho_b C_{D_b} \frac{S_b'}{S_b} v_b^2 \quad (13)$$

where $\mathrm{V}_A = \mathrm{S}_b \mathrm{P}_d$.

In the case of non-penetrative projectile (rod, [55]), the heat energy, work of friction and drag become zero, such as the resulting non-penetrative equivalent impact (13) stress has the form:

$$\sigma_{non-penetrative\ impact}^{i=1} = \frac{\rho_b v_b^2}{2} - \frac{1}{2} G_A \varepsilon_{shear,A}^2 - \frac{1}{2}\sigma_{UTS,A}\varepsilon_{plastic,A}^2 - \frac{1}{2}\sigma_{c_A}\varepsilon_{C,A}^2 - \frac{E_A \varepsilon_A^2}{2} \quad (14)$$

The non-penetrative impact stress might contribute to studies concerning soft impact [56].

2.2 *Monolithic Multi – layer (composite armor) penetration distance model*

In the multi-layer case, we have certain deceleration value (a_i) that appropriate to each armor layer ($i - layer\ index$) together with appropriate velocities for each of the entrance and the outer layer section (v_b^i, v_p^i), respectively. Accordingly, the total thickness penetration distance is:

$$\mathrm{P}_{distance}^{Multi-layer} = \sum_{i=1}^{N} \left[\frac{\left(v_b^i\right)^2 - \left(v_p^i\right)^2}{2a_i} \right] \quad (15)$$

where N represents the layers number. Hence, by manipulating (11) the total time of penetration will be:

$$\mathrm{t}_{penetration}^{Multi-layer} = \sum_{i=1}^{N} \left[\frac{v_b^i - v_p^i}{a_i} \right] \quad (16)$$

Now, the deceleration expression (3) for general i-layer case of the multi-layer model will be defined by:

$$a_i = \frac{\Delta E^i}{m_b L_b} = \frac{\left(v_b^i\right)^2 - \left(v_{p0}^i\right)^2}{2P_d^i} - \frac{\left(\rho_A C_{P_A} \Delta T_A\right)_i + \frac{1}{2}E_A^i \left(\varepsilon_A^i\right)^2 + \frac{1}{2}\sigma_{c_A}^i \left(\varepsilon_{CA}^i\right)^2 + \frac{1}{2}\sigma_{UTS,A}^i \left(\varepsilon_{plastic,A}^i\right)^2 + \frac{1}{2}G_A^i \left(\varepsilon_{shear,A}^i\right)^2 + 2\mu_k^i \rho_b g L_b}{\rho_b L_b} \quad (17)$$

where the velocities (entrance, exit) of each stage (layer) are combined from the following kinematic relations:

$$v_b^i = v_b^{i-1} - a_i t_i \quad (18)$$

$$v_{p0}^i = v_b^i - a_i t_i \quad (19)$$

Or alternatively,

$$\left(v_{p0}^i\right)^2 = \left(v_b^i\right)^2 - 2a_i \left(P_{d_i}\right) \quad (20)$$

where $a_i > 0$ since we have already implemented the negative sign of the deceleration in the kinematic model.

The equivalent impact stress will be (for example, could be useful for Ref. [57]):

$$\sigma_{impact,NDM}^i = \frac{\Delta E^i}{S_b \mathrm{P}_d} = \frac{\left(v_b^i\right)^2 - \left(v_{p0}^i\right)^2}{2} - \left(\rho_A C_{P_A} \Delta T_A\right)_i + \frac{1}{2}E_A^i \left(\varepsilon_A^i\right)^2 + \frac{1}{2}\sigma_{c_A}^i \left(\varepsilon_{CA}^i\right)^2 + \frac{1}{2}\sigma_{UTS,A}^i \left(\varepsilon_{plastic,A}^i\right)^2 + \frac{1}{2}G_A^i \left(\varepsilon_{shear,A}^i\right)^2 \quad (21)$$

In the case of non-penetrative projectile the heat energy, work of friction and drag become zero, such as Eq. (13) formula becomes as the non-penetrative equivalent impact:

$$\sigma^{i}_{non-penetraitive\ impact} = \frac{\left(v_b^{i=1}\right)^2}{2} + \frac{1}{2}E^{i}_{A}\left(\varepsilon^{i}_{A}\right)^2 + \frac{1}{2}\sigma^{i}_{c_A}\left(\varepsilon^{i}_{CA}\right)^2 + \frac{1}{2}\sigma^{i}_{UTS,A}\left(\varepsilon^{i}_{plastic,A}\right)^2 + \frac{1}{2}G^{i}_{A}\left(\varepsilon^{i}_{shear,A}\right)^2 \quad (22)$$

The latter equation might contribute to studies concerning soft impact in composite materials [24, 58].

Concerning metamaterials to enhance energy absorption of suspension component made of soft polymer core involved with ceramic outer plate, e.g. the metamaterials are engineered properties of cellular repeating materials pattern [58-59]. Based on the study done by Varma and Sarkar [59], implementing the 3-modes (bending, shear, and stretch) metamaterial energies expressions [59] into (1) together with (15) and (21)-(22), yields the physical relations that appropriate for the case of metamaterials armor penetration case.

Finally, a few words on the elastic composite armor penetration will be mentioned. One might observe that in case of armor composite elastic behavior [24, 43-52], there are four types of ballistic mechanical mechanisms: Fibres tension mechanism (e.g., Kevlar woven layer, see Figs. 16-6, 9-10 in Ref. [24]) [45-50], compression mechanism (e.g., Glass-Fibre/Epoxy composite [51-52], see Figs. 32-33 in Ref. [24]), shear mechanism (see Fig.7c in Ref. [24]) and combined tension-compression mechanism (e.g., elastic woven layer composed with Ceramics or metals layers) ([14, 19, 24]). The tension mechanism is usually involved with the woven elastic fibres (soft material [24, 51]) and tend to resist the projectile motion such as each yarn [38] is stretched [24, 38] in contrast to the case of fracture deformation (characterized rigid materials or composite layers [14, 19, 24, 43, 51 - 52]) where compressibility controls the material resistance to the projectile motion. A mono-layer proposed model might be used for the woven elastic fibres, only if equivalent macro properties data are available for the specific woven layer (transforming the yarn from micro scale to macro scale, e.g. equivalent Young modulus, maximum compressive and tensile stresses) since we have deformation behavior (unlike the fracture behavior of rigid materials), such as the tensile strength (σ_{UTS_A}) of the yarn plays main role compared to the compressive stress (but yet need to be considered). In case we have multi woven layer, then each woven layer of every (i) stage has its equivalent properties, which might be fitted to the current multi-layer model.

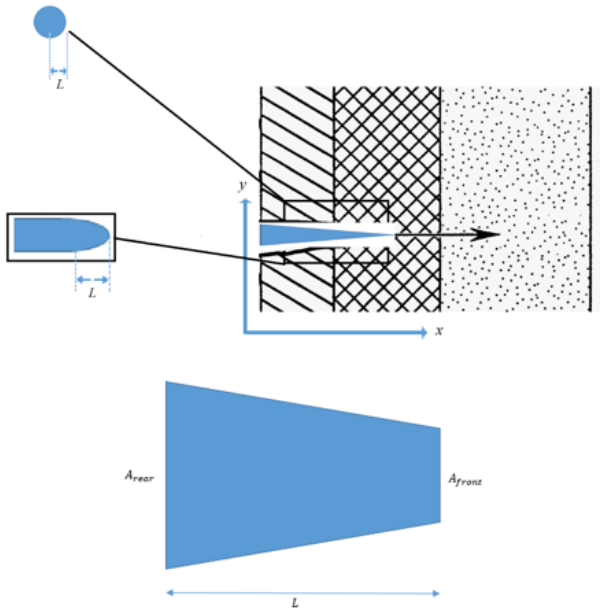

Figure 1 Bullet and erosion particle penetrative illustration in Cartesian coordinate system – mono/multi –layer (fracture mechanism).

2.3 *Composite weave-fabric Mono – layer penetration model*

In case we have laminated, composite mono-layer armor structure made from textile composition [19, 24, 45, 47, 52] such as the proposed model (2) will be revaluated by entering the yarn fiber (denoted by the subscripts letters $_{Y,A}$) energy properties alongside the generalized fabric layer as:

$$a_{Composite\ mono-layer} = \frac{v_b^2}{2\mathrm{P}_d} - \frac{\rho_A C_{P_A}\Delta T_A + \frac{1}{2}E_A\varepsilon_A^2 + \frac{1}{2}\sigma_{c_A}\varepsilon_{C,A}^2 + \frac{1}{2}\sigma_{UTS,A}\varepsilon_{plastic,A}^2 + \frac{1}{2}G_A\varepsilon_{shear,A}^2 + \rho_{Y,A}C_{P_{Y,A}}\Delta T_{Y,A} + \frac{1}{2}E_{Y,A}\varepsilon_{Y,A}^2 + \frac{1}{2}\sigma_{c_{Y,A}}\varepsilon_{C,Y,A}^2 + \frac{1}{2}\sigma_{UTS,Y,A}\varepsilon_{plastic,Y,A}^2 + \frac{1}{2}G_{Y,A}\varepsilon_{shear,Y,A}^2 + 2\mu_k\rho_b g L_b + \frac{1}{2}\frac{S_b'}{S_b}\rho_b C_{D_b}v_b^2}{\rho_b L_b} \quad (23)$$

Assuming that the Yarn strain properties are equal to the whole fabric layer properties ($\varepsilon_A = \varepsilon_{Y,A},\ \varepsilon_{C,A} = \varepsilon_{C,Y,A}, \varepsilon_{plastic,Y,A} = \varepsilon_{plastic,A}, \varepsilon_{shear,Y,A} = \varepsilon_{shear,,A}$) resulting with the following equation for deceleration in the form [19]:

$$a_{Composite\ mono-layer} = \frac{v_b^2}{2P_d} - \frac{\rho_A C_{P_A}\Delta T_A + \rho_{Y,A} C_{P_{Y,A}}\Delta T_{Y,A} + \frac{1}{2}(E_A + E_{Y,A})\varepsilon_A^2 + \frac{1}{2}\left(\sigma_{c_A} + \sigma_{c_{Y,A}}\right)\varepsilon_{C,A}^2 + \frac{1}{2}\left(\sigma_{UTS,A} + \sigma_{UTS,Y,A}\right)\varepsilon_{plastic,A}^2 + \frac{1}{2}(G_A + G_{Y,A})\varepsilon_{shear,A}^2 + + 2\mu_k \rho_b g L_b + \frac{1 S_b'}{2 S_b}\rho_b C_{D_b} v_b^2}{\rho_b L_b} \quad (24)$$

Accordingly, the appropriate equations for the desirable parameters; penetration distance, time of penetration, residual velocity, the penetrative and the non-penetrative stresses of impact will require substituting the deceleration expression (23) into the monolithic form expressions (7)-(13), respectively.

2.4 *Composite weave-fabric Multi – layer penetration model*

In more generalized case made of brittle material (monolithic) layers alongside (composed) elastic polymeric layers and alloys [12], the deceleration expression (17) will be brought by the following form:

$$a_{i_{Compsite\ multi-layer}} = \frac{\left(v_b^i\right)^2 - \left(v_{p0}^i\right)^2}{2} \left(\rho_A C_{P_A}\Delta T_A\right)_i + \frac{1}{2}E_A^i\left(\varepsilon_A^i\right)^2 + \frac{1}{2}\sigma_{C_A}^i\left(\varepsilon_{CA}^i\right)^2 + \frac{1}{2}\sigma_{UTS,A}^i\left(\varepsilon_{plastic,A}^i\right)^2 + \frac{1}{2}G_A^i\left(\varepsilon_{shear,A}^i\right)^2 + \left(\rho_{Y,A} C_{P_{Y,A}}\Delta T_{Y,A}\right)_i + \frac{1}{2}E_{Y,A}^i\left(\varepsilon_{Y,A}^i\right)^2 + \frac{1}{2}\sigma_{C_{Y,A}}^i\left(\varepsilon_{C,Y,A}^i\right)^2 + \frac{1}{2}\sigma_{UTS,Y,A}^i\left(\varepsilon_{plastic,Y,A}^i\right)^2 + \frac{1}{2}G_{Y,A}^i\left(\varepsilon_{shear,Y,A}^i\right)^2 + 2\mu_k^i \rho_b g L_b - \frac{}{\rho_b L_b} \quad (25)$$

Therefore in similar way to the previous paragraph the appropriate expressions for the relevant parameters require the deceleration expression (25) to be inserted into the multi-layer expressions (15)-(22).

Until now, four kinds of armor designs (or alternatively, the projectile design) have been proposed, as follows:

1. Sec. 2.1 concerns monolithic armor based on high strength and temperature - fracture deformation mechanism [6, 11, 26-33, 34-38, 41 - 42, 54-55, 62].

2. Sec. 2.2 concerns multi-layer monolithic armor based on high strength and temperature fracture - deformation mechanism [15, 17, 22-23, 36, 39, 41, 57].

3. Sec. 2.3 concerns weave-fabric composite armor based on elastic deformation mechanism [19, 24, 43, 45-46, 49, 56].

4. Sec. 2.4 concerns weave-fabric armor made of composite layer combination with brittle layers based on fracture mechanism alongside elastic deformation mechanism [12, 18-21, 26, 47-48, 50, 58-59]. The idea is that we have a multi-layer armor that initially reduces the projectile high temperature by absorbing the first impact stress, while the second layers protects against the developed impact wave, whereas the last layer is applied to reduce the ballistic residual velocity (alternatively, the residual mechanical stresses).

On the one hand, the differences between Sec. 2.1 and Sec. 2.2 as well as Sec. 2.3 and Sec. 2.4 configurations might be insignificant. For instance, three or four monolithic layers could be considered as (one) sole monolithic layer as compatible with configuration 2.1 [36], however, there are cases where number of layers should be considered as multilayer model [36]. Moreover, a weave-fabric composite multi-layer configuration might fit to represent configuration 2.3 in case where each fabric layer has the same properties [46]; otherwise, it might be suitable to compatible with configuration 2.4 [20, 47].

Remark that every impact process is involved with heating (cellular meta-materials, insulating

wound carbon, etc.), mechanical compressive/shear/tensile stresses (Alumina, Ceramics fibres, Graphite/Carbon fibres) and waving (damping cellular materials, rubber, Chiral-wiring materials).

Next, in the following section a comparison will be made between literature and proposed approximate analytic models.

3 Comparison between ballistic experimental results & presented theory

This section presents comparisons between literature studies and current calculations based on Eqs. (8) - (9) for two main ballistic parameters; penetration distance and time parameters that are determined by the projectile deceleration, respectively. Remark that the calculations have also been performed for the total energy (2) and penetration (5) parameters (without literature comparison due to lack of data). The comparison will concern the case of ballistic projectile of bullet and rod penetration experiments (input parameters and output data results including description of each case are well described in Tables 1-3) that have been performed on various cases of armor material vs. ballistic projectile [6, 19, 29, 34-36, 38-39, 41-42, 63] compared to the presented mono-layer scheme (Sec. 2.1 & 2.3). The deceleration for the composite fabric case was calculated using Eq. (16).

Observing Table 3 teaches us that the calculated penetration thickness results are in the same order of magnitude (good agreement) compared to numerous literature cases ([29, 36, 38, 41, 42, 73]). The maximum error was found to be 45% [34] while the minimum error was found to be 0.7% [41]. In the aspect of penetration time, the current model was found to fit qualitatively (same order of magnitude) but not numerically/quantitatively (except in cases [6, 31, 41]).

Observing parameters sensitivity – it was found that the representative armor thermal energy (heat) term ($\rho_A C_{P_A} \Delta T_A$) has meaningful contribution, especially in the monolithic armor case, in particular, the temperature difference parameter (ΔT_A) which dependent on the armor melting temperature relative to the projectile surface temperature (which itself is dependent on the projectile specific heat, velocity and its surrounding temperature). Although in the case of composite weaving fabric armor (target), the elasto-plastic properties (laminate layer and its fibres strength properties [19, 24]) have an important role (dominant) in determining the deceleration as well as other ballistic parameters due to the armor insulating properties and relatively small projectile velocities reducing ΔT_A parameter. Remark that Gunnar [62] has also mentioned the importance of using the heat relation compared or together with the stress-strain relations through his own derivations. The controlled mechanism is based on elastic deformation whilst in monolithic material is based on fracture deformation. Moreover, the notion 'melting point' in composite materials is not accurate for use. The reason is that the material become softer until most of molecules are moving freely (the molecules structure order is being highly deformed). The correct definition is to use the maximum service temperature term which allows the material to resist its deformation through highly mechanical heat stresses. Since the projectile motion continues even though the material limit did not reach its melting point, but mainly because the weakening of the yarn fiber strength. In the same manner, ductile armor plates also might use better penetration temperature accuracy definition (maximum service temperature/'softening temperature') that might be lower than the melting temperature [38]. The effective length (L_b) is an important key parameter to define the projectile geometry.

Experiments [42, 63] relating to the Tungsten alloy projectile Vs. Aluminum 6061-T6 target, and the Depleted Uranium caliber vs. MIL-DTL-12560B steel target, have shown qualitative behavior similarity (for more extension, see [64] about uranium fragmentation details and its applications [65]). Following the previous distinctions might explain the deviations (percentages error) between analytic and experimental results, expressed by the given data inaccuracies alongside the model constant parameters nature (for instance, the surrounding projectile

temperature, projectile effective length and mass are constants during the projectile penetration course). In the current study, it was assumed that the projectile deceleration as well as other parameters are constant in each layer – this assumption might influence the time of penetration and might be approved in further studies to be dependent on time and temperatures as well as non-linear mechanical properties (especially in composites and functionally graded materials). There is more room to sustain the rear reinforcement plate mechanism (regardless of penetration) that is significantly recorded for optimal utilization of the penetration plate in terms of mechanical properties [6]. Finally, the impact wave theory might also explain some of the penetration shape behavior.

To sum it up, the prominent advantage of the presented model approximation based mainly on energetic parameters (velocity, heat) and minimum number of geometry parameters.

Table 1. Penetration parameters values from literature ($note\ that\ \varepsilon_{E_A} = 1/3\varepsilon_{plastic,A}$).

Ref.	Description	ρ_A [kg/m³]	V_0^{-1} [m/sec]	$T_{room,A}$ [K]	C_{P_A} [J/kg-K]	E_A [GPa]	G_A^{-1} [GPa]	$\varepsilon_{compressive,A}^{-2}$	$\varepsilon_{shear,A}^{-2}$	$T_{melting,A}$ [K]
6	AD 85 target Vs. Steel sharp cylinder	8050	762	924.1	460	221	91	0.05	0.05	2345
19	2D plain weave E-glass fabric target Vs. Cylindrical, flat-ended hardened steel	8050	320	308.7	460	70	1.9	0.06	0.03	630
29	Ogive-nose 4340 VAR steel rod Vs. Al 6061-T6511 target	7850	821	1002.5	475	69	26	0.12	0.12	855
34	Conical Arne tool steel projectile Vs. Weldox 460 E steel targets (Test C3)	7800	206.9	339.5	460	200	80	0.17	0.17	1800
35	Conical Arne tool steel projectile Vs. AA5083-H116 target	7800	302.4	392.4	460	70	26.4	0.17	0.17	893
36	7.62AP Vs. mild steel target	7850	821	1025.7	460	203	80	0.05	0.05	1800
38	7.62AP Vs. high hardness steel target (500 HB steel)	7850	854	1085.7	460	210	80	0.04	0.04	1800
39	AK-47 Vs. ceramic target	7850	800	988.65	460	193	--	0.001	0.001	2293
41	7.62AP Vs. AL-7075 T6 target (Test no. 5)	7850	616.4	706	460	71.1	27	0.11	0.11	893
42	Tungsten alloy projectile Vs. Aluminum 6061-T6 target	17800	742	2957.3	134	70	26	0.25	0.25	925
73	Depleted Uranium (2% Mo) flat obliquity -nosed caliber Vs. MIL-DTL-12560 (BHN 331 Steel 2" – thickness dependent, Test A-IX – Shot no. 1) target [73]	18610	861.1	3713.12	117	200	75	0.09	0.09	1766

Table 2. Penetration parameters values from literature – continue from Table 1.

Ref.	ρ_A [kg/m³]	C_{P_A} [J/kg-K]	$\sigma_{UTS,A}^{-1}$ [Gpa]	$\sigma_{compressive,A}^{-2}$ [Gpa]	$\varepsilon_{plastic,A}^{-2}$	L_b [mm]	ΔT_a [K]	μ_k
6	3420	920	0.155	0.28	0.05	10	1421	0.085
19	2000	800	0.570	0.55	0.032	3	310	0.5
29	2700	897	0.31	0.24	0.12	11.8	147.52	0.47
34	7850	452	0.72	0.73	0.17	30	1460.5	0.42
35	2700	910	0.347	0.354	0.17	30	500.6	0.47
36	7850	486	0.440	0.440	0.05	7.65	774.4	0.045
38	7800	480	1.6	1.6	0.04	7.65	7143	0.045
39	3215	850	1.2	2.4	0.001	17	1304.4	0.47
41	2810	714.8	0.520	0.530	0.11	15	187.01	0.47
42	2703	900	0.31	0.24	0.25	18	2096	0.47
73	7840	470	1.11	0.24	0.09	25.4	1947.1	0.1

Table 3. Calculated time and thickness penetration values compared to literature results.

Ref.	Calculated thickness [mm]	Literature Thickness [mm]	Thickness error deviation [%]	Calculated time of penetration [μsec]	Literature time of penetration [μsec]	Time Error [%]	Calculated Deceleration [10^6-m/sec^2]	Calculated Total energy difference [10^6-J]
6	10.2	8.636	18	26.7	35.1	24	28.5	0.095
19	3.9	5	22	24.4	271	91	58.05	0.0168
29	103.4	102	1.4	251.9	--	--	3.26	0.0838
34	1.5	2.73	45	14.5	103	86	14.27	0.05245
35	12.4	16.3	24	81.61	237	66	3.705	0.1120
36	13.12	14.1 3 layers of 4.7 (thick.) [mm] each	7	31.98	--	--	25.67	0.1077
38	15.8	15.2	4	37.17	40	7	22.98	0.11655
39	23.96	30	20	59.9	50	20	13.35	0.10227
41	39.72	40 2 layers	0.7	128.88	128	0.7	4.78	0.06072
42	38.6	38.11	1.3	104.1	162	35.7	7.12	0.1995
73	48.13	50	3.74	111.8	180	37.8	7.7	1.175

4 Conclusion

In this study, we present a general framework for calculating the penetration time & thickness parameters dependent on the developed deceleration based on the projectile energy balance. A proposed model has been proposed for both mono and multi-layer cases for monolithic and composite materials, respectively. A comparison between literature experimental studies and current calculations was performed for mono-layer case for both monolithic and composite materials. Key parameters are the projectile effective length (L_b), the thermal energy and stress-strain relations that appropriate for the monolithic and composite materials, respectively. Good numerical agreement (minimum error - 0.7%, maximum error – 45%) was found for

penetration distance and time of penetration parameters (same order of magnitude). In addition, total energy and deceleration were calculated but not compared to literature results due to the lack of information. The deviations (inaccuracies) between analytic and experimental results, might be explained by the inaccuracy of the given data parameters and by the model constant nature (constant parameters during the projectile penetration course). Additionally, an equivalent to the Johnson-Cook and residual velocity semi-numerical models, a proposed impact stress and residual velocity expressions for penetrative and non-penetrative cases are exhibited, respectively. Yet, these approximations could be beneficial to understand the ballistic energy behavior of both projectile and armour parameters.

In future, the impact (energy) effect mechanism should be further study in the context of presented model in the following topics:

1. To develop improved decelerated model by making it adjustable to temperature and time dependent material properties as well as combining it with impact wave theory.

2. Building analytical and/or numerical models to explain the impact phenomena relating to high-energy projectile velocities that influence structures made of cellular chiral metamaterials (using stress-strain Gibson-Ashby relations).

3. Finding connections between micro buckling in composite materials and impact behaviour.

References:

[1] Cattell J. M., and Brimhall, D. R., "*American men of science* (3rd Ed.)". Garrison, New York: The Science Press. p. 682 (1921). doi.org/10.1038/155531a0

[2] Okun, N., "*Major Historical Naval Armor Penetration Formulae*", NavWeps website, (2017). http://www.navweaps.com/index_nathan/Hstfrmla.php#Credits

[3] Carlucci D. E., Recchia, S.S., Sproul, M., Chaplin, R., Okun, N., "Comparison of Numerical modeling of penetration of a capped projectile with a windscreen into special treatment steel with traditional formulae", *Ballistics* 30th *Int. Symp*. (2017). 10.12783/ballistics2017/16981

[4] Smith J.C., McCrackin F.L. and Scniefer H.F., "Stress-strain relationships in yarns subjected to rapid loading. Part V: wave propagation in long textile yarns impacted transversely", *Textile Research Journal* **28**, 288-302 (1958). https://journals.sagepub.com/doi/10.1177/004051755802800402

[5] Smith J.C., Blandford J.H. and Towne K.H. "Stress-strain relationships in yarns subjected to rapid loading. Part VIII: shock waves, limiting breaking velocities, and critical velocities", *Textile Research Journal* **32**, 67-76 (1962). journals.sagepub.com/doi/10.1177/004051756203200109

[6] Wilkins, M. L., "Mechanics of penetration and perforation", *International Journal of Engineering Science*, 16, 793-807 (1978). doi.org/10.1016/0020-7225(78)90066-6.

[7] Kar, A., "Residual velocity for projectiles", *Nuclear Engineering and Design* **53**, 87-95, (1979). doi.org/10.1016/0029-5493(79)90042-6.

[8] Johnson, G.R., Cook, W.H., "A constitutive model and data for metals subjected to large strains, high strain rates and high temperatures" *In: Proceedings of the 7th international symposium on ballistics, Hauge*; 541–547 (1983). scienceopen.com/document?vid=3e0958f1-d0dd-4475-a068-5dc192c6056f

[9] Zukas, J.A., *High velocity impact dynamics*, Wiley-Interscience (1990).

[10] Allen, W. A., Mayfield, E. B., and Morrison, H. L., "Dynamics of a Projectile Penetrating sand", *Journal of Applied Physics*, **28**, 370 - 376 (1957). doi.org/10.1063/1.1722750

[11] Stone G. W., "*Projectile penetration into representative targets*", Report, U.S. Sandia National Lab, SAND94- 1490, (1994). ui.adsabs.harvard.edu/abs/1994STIN...952 2726S

[12] Yadav, S., Ravichandran, G., "Penetration resistance of laminated ceramic/polymer structures", *International Journal of Impact Engineering* **28**, 557-574 (2003).

[13] Akella, K., Naik, N. K., "Composite Armour—A Review", *Journal of the Indian Institute of Science* **95**, 297-312, (2015). http://journal.library.iisc.ernet.in/index.php/iisc/article/view/4574

[14] Naik, N. K., "*Ballistic impact behavior of composites: analytical formulation*: *Ch 15: Dynamic Deformation, Damage and Fracture in Composite Materials and Structures*", Elsevier, Woodhead Publishing, 425-270 (2016). doi.org/10.1016/C2014-0-01175-6

[15] Naik, N. K., Kumar, S., Ratnaveer, D., Joshi, M. and Akella, K., ''An energy-based model for ballistic impact analysis of ceramic-composite armors", *International Journal of Damage Mechanics* **22**, 145-187 (2013). doi:10.1177/1056789511435346

[16] Neckel, L., Hotza, D., Stainer, D., Janßen, R., Lezana, A. G. R., Dias, A., and Al-Qureshi, H. A., "Solutions for Impact over Aerospace Protection", *Key Engineering Materials* **488**, 25–28. (2011). doi.org/10.4028/www.scientific.net/kem.488-489.25

[17] Neckel, L., Hotza, D., Stainer, D., Janssen, R., Al-Qureshi, H. A., "Modelling of Ballistic Impact over a Ceramic-Metal Protection System", *Advances in Materials Science and Engineering* **Article ID 698476**, 1-8 (2013). doi.org/10.1155/2013/698476

[18] Shaktivesh, N.S. Nair, Ch. V. Sesha Kumar, Naik, N. K., "Ballistic impact performance of composite targets", *Materials & Design* **51**, 833-846 (2013). doi.org/10.1016/j.matdes.2013.04.093.

[19] Shaktivesh, N. S. Nair and Naik N. K., "Ballistic impact behavior of 2D plain weave fabric targets with multiple layers: Analytical formulation", *International Journal of Damage Mechanics*, **24**, 116-150 (2015). dx.doi.org/10.1177/1056789514524074

[20] Phadnis *et al*., "Ballistic damage in hybrid composite laminates", *Journal of Physics*: Conference Series **628,** 012092 (2015). doi.org/10.1088/1742-6596/628/1/012092

[21] Luz, Fernanda Santos da, Lima Junior, Edio Pereira, Louro, Luis Henrique Leme, & Monteiro, Sergio Neves, "Ballistic Test of Multilayered Armor with Intermediate Epoxy Composite Reinforced with Jute Fabric" *Materials Research* **18**, 170-177 (2015). dx.doi.org/10.1590/1516-1439.358914

[22] Rahman, N. A., Abdullah, S., Zamri, W. F. H., Abdullah, M. F., Omar, M. Z., & Sajuri, Z., "Ballistic Limit of High-Strength Steel and Al7075-T6 Multi-Layered Plates Under 7.62-mm Armour Piercing Projectile Impact". *Latin American Journal of Solids and Structures* **13**, 1658-1676 (2016). dx.doi.org/10.1590/1679-78252657

[23] Kumar, S., Akella, K., Joshi, M. *et al*. Performance of Ceramic-Composite Armors under Ballistic Impact Loading. *J. of Materi Eng and Perform* **29,** 5625–5637 (2020). doi.org/10.1007/s11665-020-05041-z

[24] Abtew, M. A., Boussu, F., Bruniaux, P., Loghin, C., Cristian, I., "Ballistic impact mechanisms – A review on textiles and fibre-reinforced composites impact responses", *Composite Structures* **223**, 110966 (2019). doi.org/10.1016/j.compstruct.2019.110966.

[25] Murr L.E. *Ballistic and Hypervelocity Impact and Penetration. In: Handbook of Materials Structures, Properties, Processing and Performance*, Springer, Cham. (2015). doi.org/10.1007/978-3-319-01815-7_49

[26] El Messiri, M., *Protective armor engineering design*, Taylor & Francis, Apple Academic Press Inc. (2020). doi.org/10.1201/9780429057236

[27] Yarin A. L., Rubin M. B., Roisman I. V., "Penetration of a rigid projectile into

an elastic-plastic target of finite thickness", *International Journal of Impact Engineering*, **16**, 801-831, (1995).

[28] Ben-Dor, G., Dubinsky, A., and Elperin, T. "Ballistic Impact: Recent Advances in Analytical Modeling of Plate Penetration Dynamics–A Review" *ASME. Appl. Mech. Rev.* **58**, 355–371 (2005). doi.org/10.1115/1.2048626

[29] Piekutowski, A. J., Forrestal, M. J., Poormon, K. L., Warren, T. L., "Penetration of 6061-T6511 aluminum targets by ogive-nose steel projectiles with striking velocities between 0.5 and 3.0 km/s", *International Journal of Impact Engineering* **23**, Part 2, 723-734 (1999). doi.org/10.1016/S0734-743X(99)00117-7

[30] Rosenberg, Z., Dekel, E., "Revisiting the perforation of ductile plates by sharp-nosed rigid projectiles", *International Journal of Solids and Structures*, 47, 3022-3033 (2010).

doi.org/10.1016/j.ijsolstr.2010.07.003

[31] Z. Rosenberg, E. Dekel, "The penetration of rigid long rods – revisited", *International Journal of Solids and Structures* **36**, 551-564 (2009). doi.org/10.1016/j.ijsolstr.2009.07.027

[32] Z. Rosenberg, E. Dekel, "On the deep penetration and plate perforation by rigid projectiles", *International Journal of Solids and Structures* **46**, 4169-4180 (2009). doi.org/10.1016/j.ijsolstr.2009.07.027

[33] Yossifon, G. Rubin, M. B., Yarin, A. L., "Penetration of a rigid projectile into a finite thickness elastic–plastic target — comparison between theory and numerical computations", *International Journal of Impact Engineering* **25**, 265-290, 2001, doi.org/10.1016/S0734-743X(00)00040-3.

[34] Børvik, T., Langseth, M., Hopperstad, O. S., Malo, K. A., "Perforation of 12mm thick steel plates by 20mm diameter projectiles with flat, hemispherical and conical noses: Part I: Experimental study", *International Journal of Impact Engineering* **27**, 19-35 (2002). doi.org/10.1016/S0734-743X(01)00034-3

[35] Børvik, T., Clausen, A. H., Hopperstad, O. S., Langseth, M., "Perforation of AA5083-H116 aluminium plates with conical-nose steel projectiles—experimental study", *International Journal of Impact Engineering* **30**, 367-384, (2004). doi.org/10.1016/S0734-743X(03)00072-1

[36] Senthil, K., Iqbal, M., Gupta, N., "Ballistic resistance of mild steel plates of various thicknesses against 7.62 AP projectiles", *International Journal of Protective Structures* **8**, 177-198 (2017). doi:10.1177/2041419617700007

[37] Stewart, M. G., Netherton, M. D. "Statistical variability and fragility assessment of ballistic perforation of steel plates for 7.62 mm AP ammunition", *Defence Technology* **16**, 503-513, (2020).

doi.org/10.1016/j.dt.2019.10.013.

[38] Kılıç, N., Ekici, B., "Ballistic resistance of high hardness armor steels against 7.62mm armor piercing ammunition", *Materials & Design* **44**, 35-48 (2013). doi.org/10.1016/j.matdes.2012.07.045.

[39] Shakoor A., Khan, N., Muhammad, R., Ahmed, N., Silberschmidt, V. V., "*Finite Element Simulation of Bullet Resistant Composite Body Armor*", Fourth International Conference on Aerospace Science & Engineering (ICASE), 2015.

[40] Soriano-Moranchel, F. A., Sandoval-Pineda, J.M., Gutiérrez-Paredes, G.J., Silva-Rivera, U.S., Flores-Herrera, L.A., "Simulation of Bullet Fragmentation and Penetration in Granular Media" *Materials* **13**, 5243 (2020). doi.org/10.3390/ma13225243

[41] Forrestal, M. J., Børvik, T. and Warren, T.L. "Perforation of 7075-T651 Aluminum Armor Plates with 7.62 mm APM2 Bullets", *Exp. Mech.* **50**, 1245–1251 (2010). doi.org/10.1007/s11340-009-9328-4

[42] Manes, A., Serpellini, F., Pagani, M., Saponara, M., Giglio, M., "Perforation and penetration of aluminum target plates by armour piercing bullets", *International Journal of Impact Engineering* **69**, 39-54 (2014). doi.org/10.1016/j.ijimpeng.2014.02.010

[43] Shanazari, H., Liaghat, G., Feli, S., Hadavinia, H., "Analytical and experimental study of high-velocity impact on ceramic/nanocomposite targets". *Journal of Composite Materials* **51**, 3743-3756 (2017). 10.1177/0021998317692658

[44] Song, B., Park, H., Lu, W., and Chen, W., "Transverse Impact Response of a Linear Elastic Ballistic Fiber Yarn" *ASME. J. Appl. Mech*. **78**, 051023 (2011). doi.org/10.1115/1.4004310

[45] Pandya, K., Kumar, C.V.S., Nair N, Patil, P., Naik N., "Analytical and experimental studies on ballistic impact behavior of 2D woven fabric composites" *International Journal of Damage Mechanics* **24**, 471-511 (2015). doi:10.1177/1056789514531440

[46] Yang, E. C., Ngo, T. D., Ruan, D., and Tran, P., "Impact Resistance and Failure Analysis of Plain Woven Curtains" *International Journal of Protective Structures* **6**, 113–136 (2015). doi.org/10.1260/2041-4196.6.1.113

[47] Yang, E. C., Ngo, T. D., Tran, P., "Influences of weaving architectures on the impact resistance of multi-layer fabrics", *Materials & Design* **85**, 282-295 (2015) doi.org/10.1016/j.matdes.2015.07.014

[48] Dobb, M. G., Robson, R. M., and Roberts, A. H., "The ultraviolet sensitivity of Kevlar 149 and Technora fibres" *J Mater Sci* **28**, 785–788 (1993). doi.org/10.1007/BF01151257

[49] Nilakantan, G., Gillespie, J. W., Yarn pull-out behavior of plain woven Kevlar fabrics: Effect of yarn sizing, pullout rate, and fabric pre-tension, *Composite Structures* **101**, 215-224 (2013). doi.org/10.1016/j.compstruct.2013.02.018

[50] Nilakantan, G., Nutt, S., "Effects of clamping design on the ballistic impact response of soft body armor", *Composite Structures* 108, 137-150 (2014). doi.org/10.1016/j.compstruct.2013.09.017

[51] Bibo, G. A., Hogg, P. J., "Influence of reinforcement architecture on damage mechanisms and residual strength of glass-fibre/epoxy composite systems", *Composites Science and Technology* **58,** 803-813 (1998). doi.org/10.1016/S0266-3538(97)00055-9

[52] Thanomsilp, C., Hogg, P. J., "Penetration impact resistance of hybrid composites based on commingled yarn fabrics", *Composites Science and Technology* **63**, 467-482 (2003). doi.org/10.1016/S0266-3538(02)00233-6

[53] Braga F.O., Bolzan, L. T., Lima Jr., E. P., Monteiro, S. N., "Performance of natural curaua fiber-reinforced polyester composites under 7.62 mm bullet impact as a stand-alone ballistic armor". *J Mater Res Technol*. **6**, 323-328 (2017). http://dx.doi.org/10.1016/j.jmrt.2017.08.003

[54] Johnson, G. R., Cook, W. H., "Fracture Characteristics of Three Metals Subjected to Various Strains, Strain rates, Temperatures and Pressures", *Engineering Fracture Mechanics* **21**, 31–48 (1985). doi.org/10.1016/0013-7944(85)90052-9

[55] Dou, Y, Liu, Y, & Hammi, Y. "Comparison of Johnson-Cook Model and an ISV Plasticity Damage Model in Penetration Simulation." *Proceedings of the ASME 2016 International Mechanical Engineering Congress and Exposition. Volume 9: Mechanics of Solids, Structures and Fluids; NDE, Diagnosis, and Prognosis*. Phoenix, Arizona, USA. 1-6 (2016).

doi.org/10.1115/IMECE2016-68195

[56] Mirkhalaf, M., Sunesara, A., Ashrafi, B., Barthelat, F., "Toughness by segmentation: Fabrication, testing and micromechanics of architectured ceramic panels for impact applications", *International Journal of Solids and Structures* **158**, 52-65 (2019). doi.org/10.1016/j.ijsolstr.2018.08.025.

[57] Pereira, A. C., de Oliveira Braga, F., Monteiro, S. N., de Azevedo, T. M., & Braga, W. S., "Microstructural Evaluation of a 5052 H34 Aluminum Alloy Used in Multilayered Armor". *Materials Science Forum*, **930**, 513–519 (2018). doi.org/10.4028/www.scientific.net/msf.930.513

[58] Novak, N., Vesenjak, M., Kennedy, G., Thadhani, N. and Ren, Z., "Response of Chiral Auxetic Composite Sandwich Panel to Fragment Simulating Projectile Impact", *Phys. Status Solidi B* **257**, 1900099 (2020). doi.org/10.1002/pssb.201900099

[59] Varma, T.V., Sarkar, S. "Designing polymer metamaterial for protective armor: a coarse-grained formulation", *Meccanica* **56**, 383–392 (2021).doi.org/10.1007/s11012-020-01201-6

[60] Horsfall, I., Buckley, D., "The effect of through-thickness cracks on the ballistic performance of ceramic armour systems", *International Journal of Impact Engineering* **18**, 309-318 (1996). doi.org/10.1016/0734-743X(96)89051-8

[61] Hetherington, J. G., and Rajagopalan, B. P. "An investigation into the energy absorbed during ballistic perforation of composite armours", *International Journal of Impact Engineering* **11**, 33-40 (1991).

[62] Gunnar, W., "*Projectile Penetration and Perforation* 3rd Ed.", ISBN 978-91-637-7579-6, *E-Book*, (2016).

[63] Hopson, J. W., Hantel, L. W., Sandstorm, D. J., "*Evaluation of Depleted-Uranium Alloys for Use in Armor-Piercing Projectiles (U)*", Los Alamos Sci. Laboratory Report, LA - 5238, Los Alamos, New Mexico 87544 (1984).

[64] Zhu, F-L., Chen, Y., Zhu, G., L., "Numerical simulation study on penetration performance of depleted Uranium (DU) alloy fragments", *Defence Technology* **17**, 50-55 (2020). doi.org/10.1016/j.dt.2020.01.002

[65] Sandstorm, D. J., "Armor: Anti-ARMOR materials by design", 36-50, *Los Alamos Science Summer*, 36-50 (1989).

Conflict of interest statement

On behalf of all authors, the corresponding author states that there is no conflict of interest

Contribution of individual authors to the creation of a scientific article (ghostwriting policy)

The author' own fully creation.

Follow: www.wseas.org/multimedia/contributor-role-instruction.pdf

Creative Commons Attribution License 4.0 (Attribution 4.0 International , CC BY 4.0)